Advanced Materials '93, I / B: Magnetic, Fullerene, Dielectric, Ferroelectric,
Diamond and Related Materials, edited by M. Homma et al.
Trans. Mat. Res. Soc. Jpn., Volume 14B
© 1994 Elsevier Science B.V. All rights reserved.

Growth and Properties of Buckybundles

X.K. Wang, X.W. Lin, V.P. Dravid, J.B. Ketterson, and R.P.H. Chang

Materials Research Center, Northwestern University
2145 Sheridan Road, Evanston, IL 60208, USA

Buckybundles (bundles of buckytubes), approximately 50 micrometers in diameter and one centimeter in length, have been observed in a deposited carbon rod on the cathode electrode of a DC arc. Scanning electron microscopy (SEM) images clearly show an evenly spaced array of parallel buckybundles. High resolution electron microscopy (HREM) reveals that each buckybundle consists of closely packed buckytubes with their axes parallel to the bundle axis. Within each bundle it is estimated that there are about 10^6 buckytubes with diameters in the range of 40Å - 300Å. We have measured the deposited rod growth rate as a function of the He gas pressure and have evaluated the influence of the graphite feed rod diameter on the yield of buckybundles. The magnetic susceptibilities both parallel and perpendicular to the bundle axes were measured. The results show that the bundles have anisotropic diamagnetic properties. In addition, we will report the relationship between buckytube and buckyball formations.

1. INTRODUCTION

Since the first observation of carbon nanotubules by Iijima et al[1] and the synthesis of carbon nanotubules in large quantities by Ebbesen and Ajayan[2], there has been a surge of interest in the study of the properties of these nanotubules. Theoretical calculations have been carried out by several research groups to study the electronic properties of nanotubules.[3,4,5] In particular, Hamada et al[6], using tight-binding band-structure calculations, have predicted that carbon nanotubules exhibit striking variations in electronic transport, from metallic to semiconducting with narrow and moderate band gaps, depending on the diameter of the tubule and on the degree of helical arrangement of the carbon hexagons.

Based on computer simulations, Pederson and Broughton[7] have predicted that open ended nanotubules may be filled with liquids by capillary suction. Ajayan and Iijima have, in fact, observed the filling of liquid lead in nanotubules.[8] More recently, Seraphin et al have succeeded in placing yttrium carbide into nanotubules.[9] In order to encapsulate material into the nanotubes, it is necessary to first open the otherwise capped ends of the nanotubules. An oxidation process has recently been developed to open the end caps of the nanotubules and strip the outer layers of multiply wrapped tubules.[10,11]

Here we report the observation of buckybundles with approximately 50μm diameter and 1 cm long, the speculation on the formation mechanism of the bundles, and the magnetic properties of the buckytubes.

2. SYNTHESIS AND CHARACTERIZATION

The DC arc system that we use to produce bundles of buckytubes and their derivatives is the same system which is being used to generate soot for the separation of C_{60}, C_{70}, and higher fullerenes. The main difference, however, is that soot is collected from the arc chamber walls, while the buckytubes are collected from the residues on the cathode electrode of the arc.[12]

The arc was generated by a DC current (50-300A, 10-30 V) in a He atmosphere at pressures of 50-760 Torr. The electrodes of the arc consist of two graphite rods placed about 1 mm apart. The feed rod (anode) was nominally 12.7mm in diameter and 305mm long; the cathode rod was 25.4mm in diameter and 100mm long (it remains largely uneroded as the feed rod is consumed). Typical rod temperature near the arc is in range of 3000K to 4000K[13]. After arc-discharging for an hour, a deposited carbon rod 165mm in length 16mm in diameter builds up on the end of cathode. The deposition rate is 46μm/sec. The cross section of the deposited rod consists of three regions (a gray core, a black ring, and a gray shell) as shown in Fig. 3(a). The density of the deposited rod is measured to be 2.022 g/cm^3. The total yield is at least several grams per hour.

Scanning electron microscopy (SEM) observations were performed on a bulk sample taken from the

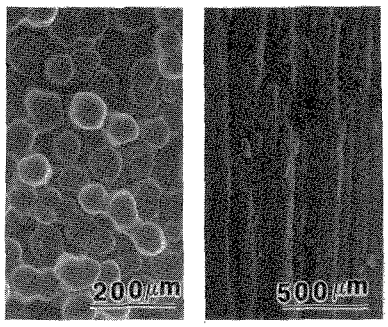

Fig. 1 - SEM micrographs of a bulk buckybundle sample, showing an evenly spaced array of parallel buckybundles (a) end-on view, (b) side view.

black region of a deposited rod. A sequence of SEM micrographs is shown in Fig. 1, which clearly exhibits an array of rather evenly spaced, parallel, and closely packed bundles, several ten's microns in diameter and about one centimeter in length as a major constituent of the black region in the deposited rod.

Both cross-sectional and high resolution electron microscopy (HREM) images of the oriented, parallel bundles are shown in Fig. 2(a) end-on view and (b) side view of a single bundle. These micrographs directly reveal that a bundle consists of buckytubes, running parallel to one another. Since the name "buckytubes" seems to have been adopted, it is natural to call the new structure a "buckybundle". In Fig. 2(a) we note that although nanoscale buckytubes have a wide range of diameters (20 Å - 300 Å), they tend to pack in a parallel, closely packed structure. Since the valence requirements of all atoms in a buckytube (with two sealed ends) are satisfied, the interaction among graphite tubes should be van der Waals in nature. Therefore, it is energetically favorable for buckytubes packed closely together to form a buckybundle.

To explore the growth conditions and understand the nucleation and growth mechanism, graphite feed rods with 12.7mm, 10mm, and 8mm in diameter as well as a hollow graphite rod with an inner diameter of 6mm and an outer diameter of 12.7mm were used as anodes. An arc current density of 1.4 A/mm^2 was chosen for all of anodes, the He pressure was 450 Torr. Photographs of cross sections of the deposited rods are shown in Fig. 3. Photos (a), (b), (c),and (d) were taken from deposited rods produced by consuming graphite rods with diameters of 12.7mm, 10mm, and 8mm and the hollow rod, respectively. The graphs show that the deposited rod resulting from the 10mm graphite rod contains a smaller gray core than that 12.7mm rod. The deposited rod produced by the 8mm graphite rod has a black core and only a very thin gray shell and produced the highest yield of buckybundles. Surprisingly, no black region was observed in the hollow deposited rod.

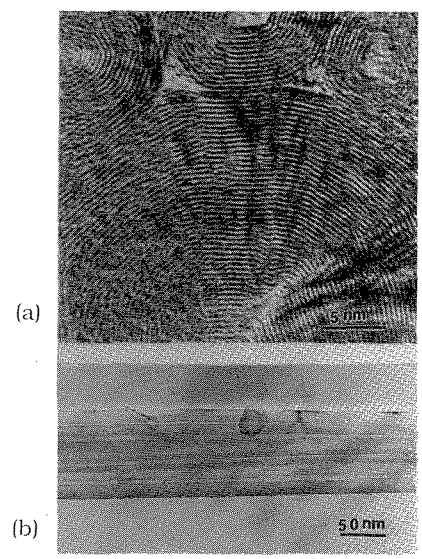

Fig. 2 (a) A cross sectional TEM image of buckybundles, (b) An HREM image of a single buckybundle consisting of buckytubes with their axes parallel to the bundle axis.

It is natural to ask why the geometry of the graphite electrodes plays so large a role in determining the distribution of buckybundles. To address this question we measured the continuity of the arc discharge using a Hewlett-Packard 7090A Measurement Plotting System. The resultant spectra demonstrate that the arc discharge is a transient process. The intensity and duration time of the arc currents fluctuate in time. An average arc-jump frequency of about 10 Hz was observed. One can conjecture that the arc discharge starts at a sharp edge near the point of closest approach, and after vaporizing this region it jumps to what then becomes the next point (usually about the radius of the arc area) of closest approach and so on. The arc wanders around on the surface of the end of the anode leading, on the average, to a quasi-continuous evaporation.

From this point of view, we may speculate on the influence of the geometry on the distribution of the buckybundles shown in Fig. 3. For the 12.7 mm diameter rod, the arc discharge builds up at the edge of the rod end, and then moves along the edge as a quasi-continuous discharge. The highest temperature occurs between the center and the edge of the rod, where the black ring is observed, as shown in Fig. 3 (a). The temperature at the core region and the outer shell, where gray amorphous carbon is located, is high enough to form amorphous carbon confirmed by HREM, but is not sufficient for the black materials to form. For the 10mm diameter rod, the highest temperature is closer to the center of the rod. We speculate that this is why the gray core is smaller than for the 12.7mm rod. For the 8mm diameter rod, the highest temperature should be at center of the rod. Only the black region and a thin gray shell show up in the cross section of the deposited rod. In this case, the total yield of buckybundles as a proportion of the graphite rod is optimal. For the hollow rod, the hole at the center of the rod allows heat to radiate (or conduct via the He gas) along the rod axis providing an additional cooling channel. The temperature produced by the arc discharge, with the same current density and under the same He pressure, may not be high enough for the buckybundles to form. From these results, we may conclude that the temperature is one of key factors in formation of the buckybundles and the formation of the bundles requires a higher temperature than that for amorphous carbon.

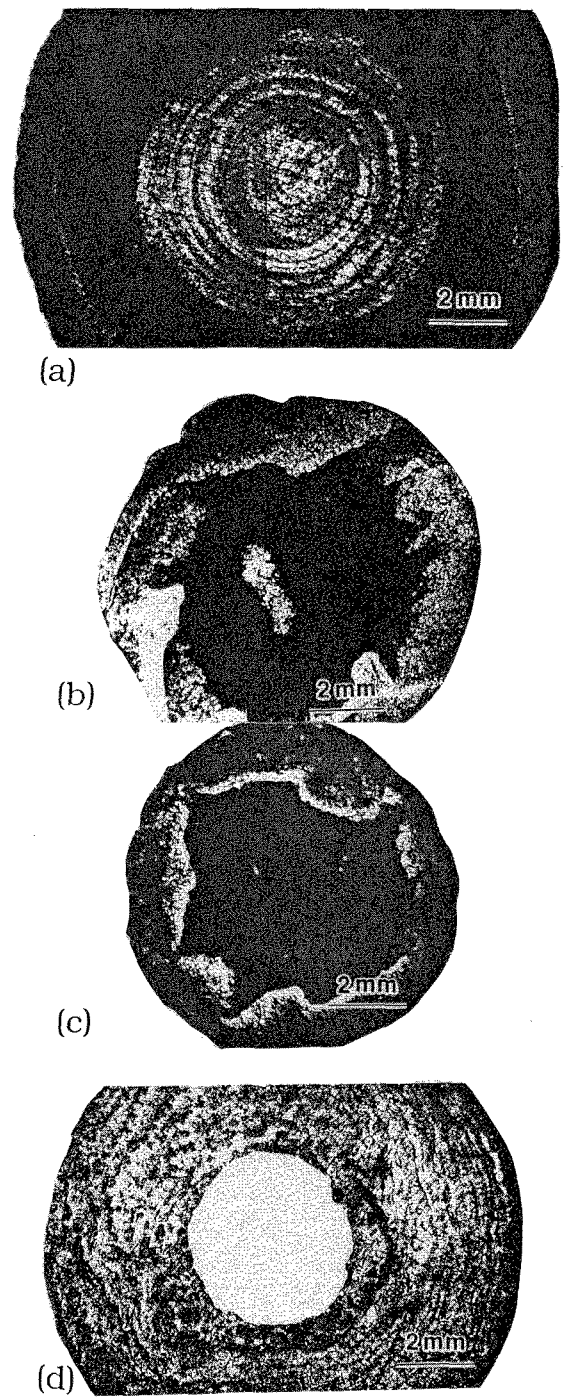

Fig. 3 - Photographs of cross sections of the deposited rods and the hollow anode.

We have speculated that buckytubes may be a much more efficient precursor for buckyball (C_{60}) and higher fullerene formation. Buckytubes in the close vicinity of the arc might become fragmented in a

manner that would result in short length (capped or uncapped) buckytubes. These short segments of buckytubes (linear dimension roughly equal to their diameter) may escape the graphite rod and close in a variety of ways. Those buckytube fragments, which have the critical number of carbon atoms as well as the number of hexagons and pentagons, may eventually form closed shell fullerenes of 60 or more carbon atoms. Those that do not satisfy the number of carbon atoms or hexagon-pentagon criteria or both may dissociate rapidly to form other carbon residues that form during fullerene synthesis.

To substantiate our hypothesis that buckytubes may be a more efficient precursor for buckyball formation, we performed the following comparison experiments. Separate batches of soot were generated with two different starting anode rods, a standard graphite rod and a redeposited residue rod with a substantial amount of buckytubes present. The fraction C_{60} was separated from the soot using a standard recirculating Wudl system. For the graphite rod, the soot contained ~10% C_{60}. For residue rods with buckytubes, the percentage yield of C_{60} was in the range of 20 to 60%, depending on the percentage of buckytubes present in the rod. The relative amount of higher fullerene (greater than C_{70}) has also increased from our soot separation. The fullerene yield correlated well with the number density of buckytubes in the residue rod, that is, the larger the number of buckytubes, the more the yield of fullerenes.

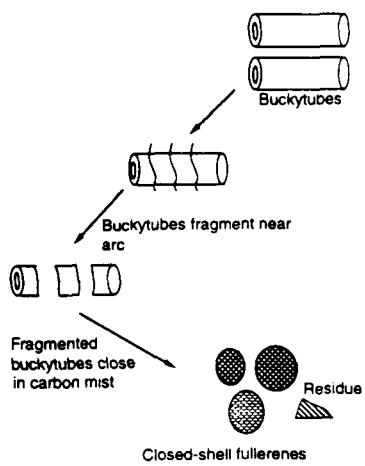

Fig. 4 - Schematic illustration of the formation of buckyballs via buckytubes.

The possible steps in closed shell fullerene formation are outlined in Fig. 4. The first step includes tearing of graphite sheets in the vicinity of the arc. The folding of the graphite sheets would lead to buckytube formation.

Magnetic susceptibility measurements were performed using a magnetic property measurement system (Quantum Designs Model MPMS). This system has a differential sensitivity of 10^{-8} emu in magnetic fields ranging from -5.5T to +5.5T over a temperature range of 1.9K-400K. The materials studied included: three buckybundle samples of 0.0712g, 0.0437g, and 0.0346g; 0.0490g of C_{60} powder, 0.1100g of gray-shell materials, 0.1413g of polycrystalline graphite anode, and an 0.0416g graphite single crystal. Measurements were performed at temperature from 2K to 300K and in magnetic fields ranging from 50G to 4T.

The susceptibility of buckytubes was measured with the magnetic field (H) either parallel to ($\chi^{\parallel}_{B}$) or perpendicular to ($\chi^{\perp}_{B}$) the tube axis. All samples used in this work were enclosed in gelatin capsules, and the background of the container was subtracted from the data. The absolute accuracy of the mass susceptibility relative to the"standard" value of the graphite crystal is about 1%.

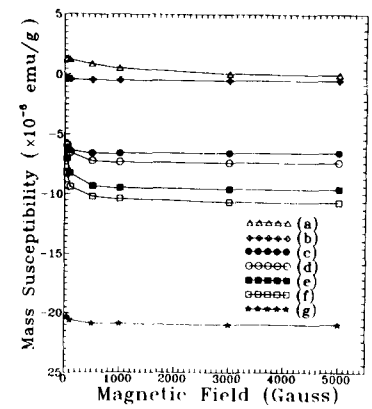

Fig. 5 - Magnetic field dependence of the susceptibilities measured at a temperature of 300K: (a) graphite: c-axis perpendicular to H, (b) C_{60} powder, (c) polycrystalline graphite anode, (d) gray-shell materials, (e) buckytube: axis perpendicular to H, (f) buckytube: axis parallel to H, and (g) graphite: c-axis parallel to H.

The measured mass susceptibility values for buckytubes (both $\chi^{\perp}_{B}$ and $\chi^{\parallel}_{B}$), C_{60}, the gray-shell materials, the polycrystalline graphite anode, and the graphite crystal are shown in Fig. 5 as a function of the magnetic field at a temperature of 300K. The curves show that, except for C_{60} the room-temperature susceptibilities are independent of magnetic field for fields larger than 3000G. The measured susceptibility values are shown in Table 1.

The measured room temperature magnetic susceptibility of a bulk sample of buckytubes is -10.75 x 10^{-6} emu/g for the magnetic field parallel to the tube axes, which is approximately 1.1 times the perpenducular value and 30 times larger than that of C_{60}.

The measured mass susceptibility of -0.35x10^{-6} emu/g for C_{60} is consistent with the literature value[15]. The C_{60} powder shows the strongest exhibit diamagnetism until H is greater than 5000G; saturation is observed for fields greater than 3T. The C_{60} results, involving a very small diamagnetic susceptibility and a strong magnetic field dependence, appear to support the Elser-Haddon[16,17] result where a cancellation occurs between the diamagnetic and paramagnetic contributions. The small measured susceptibility of C_{60} suggests that if it (or possibly other fullerenes) is present as a contaminant in the buckybundle matrix (which is likely at some level) its contribution will be small.

Table 1 Measured room-temperature susceptibilities.

Material	Symbol	Susceptibility X 10^{-6} emu/g
buckytube: axis parallel to H	$\chi^{\parallel}_{B}$	-10.75
buckytube: axis perpendicular to H	$\chi^{\perp}_{B}$	- 9.60
C_{60} powder	χ_{C60}	- 0.35
polycrystalline graphite anode	-	- 6.50
gray-shell material	-	- 7.60
graphite: c-axis parallel to H	$\chi^{\parallel}_{G}$	-21.10
graphite: c-axis perpendicular to H	$\chi^{\perp}_{G}$	- 0.50

We see from Fig. 5 that the measured susceptibility of the polycrystalline graphite anode (used to produce the fullerenes measured here) is -6.50 x 10^{-6} emu/g, which is near the literature value (implying the behaviors of the remaining materials do not involve impurities arising from the source material). The measured susceptibility of the gray-shell material, which consists of amorphous carbon mixed with fragments of buckytubes and buckydoughnuts, is close to (but larger than) that of the source rod.

We concluded from these measurements that buckytubes have a large diamagnetic susceptibility for H both parallel to and perpendicular to the tube axes. We attribute the large susceptibility of the buckytubes to de-localized electrons in the graphite sheet. The increase in the diamagnetism at low temperature is attributed to a rise from an increasing mean free path. C_{70}, which is formed by 12 pentagons and 25 hexagons, exhibits a larger diamagnetic susceptibility than that of C_{60}, which consists of 12 pentagons and 20 hexagons. This suggests that the diamagnetic susceptibility of fullerenes may increase with an increasing fraction of hexagons. The susceptibility of the buckytubes is likely the largest in this family.

REFERENCES

1 S. Iijima, *Nature*, **354**, 56 (1991).

2 T.W. Ebbesen and P.M. Ajayan, *Nature*, **358**, 220 (1992).

3 Kazuyoshi Tanaka, Kenji Okahara, Mayumi Okada, Tokio Yamabe, *Chem. Phys. Letters*, **Vol 191:No. 5**, pg. 469-472, (April 10, 1992).

4 J.W. Mintmire, B.I. Dunlap, C.T. White, *Am. Phys. Society*, **Vol 68:No. 5**, pg. 631-34, (February 3, 1992).

5 M.S. Dresselhaus, G. Dresselhaus, R. Sato, *Phys Rev. B*, **45**, 6234 (1992);R. Sato *et al., ibid,* **46**, 1804 (1992).

6 Noriaki Hamada, Shin-ichi Sawada, Atsushi Oshiyama, *Am. Phys. Society*, **Vol 68:No. 10**, pg. 1579-1581, (March 9, 1992).

7 Mark R. Pederson, Jeremy Q. Broughton, *Physical Review Letters*, **Vol 69:No. 18**, pg. 2689-2692 (November 1, 1992).

8 P.M. Ajayan, Sumio Iijima, *Nature*, **361**, pg. 333-334, (January 28, 1993).

9 Supapan Seraphin, Dan Zhou, Jun Jiao, James C. Withers, Raouf Loutfy, *Nature*, **362**, pg. 503 (April 8, 1993).

10 P.M. Ajayan, T.W. Ebbesen, T. Ichihashi, S. Iijima, K. Tanigaki & H. Hiura, *Nature*, **362**, pg. 522-525, (April 8, 1993).

11 S.C. Tsang, P.J.F. Harris, M.L.H. Green,

Nature, **362**, pg. 520-522, (April 8, 1993).

12 X.K. Wang, X.W. Lin, V.P. Dravid, J.B. Ketterson, R.P.H. Chang, *Appl. Phys. Lett.* **62**, 1881, (1993).

13 Y. Saito, M. Tomita, and T. Hayashi, MRS Fall Meeting, Boston, Nov.30-Dec.4, (1992).

14 V.P. Dravid, X. Lin, Y. Wang, X.K.Wang, A. Yee, J.B. Ketterson, R.P.H. Chang, *Science*, **259**, 1601 (1993).

15 R.S. Ruoff, D. Beach, J. Cuomo, T. McGuire, R.L. Whetten, and F. Diederich, *J. Phys. Chem.*, **95**, 3457 (1991).

16 R.C. Haddon, L.F. Schneemeyer, J.V. Waszczak, S.H. Glarum, R. Tycko, G. Dabbagh, A.R. Kortan, A.J. Muller, A.M. Mujsce, M.J. Rosseinsky, S.M. Zahurak, A.V. Makhija, F.A. Thiel, K. Raghavachari, E. Cockayne, and V. Elser, *Nature*, **350**, 46 (1991).

17 A. Pasquarello, M. Schluter, R.C. Haddon, *Science*, **257**, 1660 (1992).